JOURNAL OF SOLID STATE CHEMISTRY **137,** 174–180 (1998)
ARTICLE NO. SC987750

# A $^{151}$Eu Mössbauer Spectroscopic and Magnetic Susceptibility Investigation of the Intermetallic Compounds Eu*T*In (*T* = Zn, Pd, Pt, Au)

Ralf Müllmann,* Bernd D. Mosel,* Hellmut Eckert,*,[1] Gunter Kotzyba,† and Rainer Pöttgen†,[1]

*Institut für Physikalische Chemie, Universität Münster, Schloßplatz 4/7, D-48149 Münster, Germany; and †Anorganisch-Chemisches Institut, Universität Münster, Wilhelm-Klemm-Straße 8, D-48149 Münster, Germany

Received August 14, 1997; accepted January 9, 1998

**The title compounds were investigated by magnetic susceptibility measurements and $^{151}$Eu Mössbauer spectroscopy. EuZnIn and EuPtIn show Curie-Weiss behavior above 60 K with experimental magnetic moments of 7.80(5) and 8.0(1) $\mu_B$/Eu, respectively, indicating divalent europium. The zinc compound orders antiferromagnetically at $T_N = 8.0(5)$ K and no field induced transition is observed. EuPtIn orders antiferromagnetically in small external fields at 16.0(5) K and two metamagnetic transitions are detected at the critical field strengths $B_{C1} = 1.1(1)$ T and $B_{C2} = 2.6(2)$ T. At 5 K the saturation magnetic moment amounts to 7.0(1) $\mu_B$/Eu, suggesting a full parallel spin alignment. EuPdIn and EuAuIn order antiferromagnetically at 13.0(5) and 21.0(5) K in low external magnetic fields, respectively. The four compounds are metallic conductors. The Mössbauer measurements of the Eu*T*In compounds show $^{151}$Eu isomer shifts typical of divalent europium. The isomer shifts are found to be linearly correlated with the closest Eu–Eu distance in the structure. Based on the Mössbauer data the onset of magnetic order is observed at $T_N$(EuZnIn) = 9.5(5) K, $T_N$(EuPdIn) = 15.5(5) K, $T_N$(EuAuIn) = 20.0(5) K, and $T_N$(EuPtIn) = 20.0(5) K, respectively. The magnetically split spectrum of EuZnIn reveals evidence of Eu site inequivalence.** © 1998 Academic Press

*Key Words:* **$^{151}$Eu Mössbauer spectroscopy, intermetallic europium compounds**

## INTRODUCTION

We have recently investigated a whole series of equiatomic intermetallic Eu*TX* compounds (*T* = post transition metal; *X* = Ge, In, Sn) which exhibit a large variety of magnetic properties (1–3 and Refs. therein). Most of these intermetallics crystallize with the $KHg_2$ type structure (4) or ternary ordered derivatives like the TiNiSi type (5), the EuAuGe type (1, 6) or the EuAuSn type (3). In our previous studies on the indium compounds we mainly focused on the crystal chemistry of these fascinating materials (2, 7). We have now extended these investigations with respect to the physical properties. Herein we report about $^{151}$Eu Mössbauer spectroscopic measurements of EuZnIn, EuPdIn, EuPtIn, and EuAuIn. Additionally we investigated the magnetic and electrical properties of EuZnIn and EuPtIn. Susceptibility and resistivity data for EuPdIn and EuAuIn are reported in Ref. (7).

## EXPERIMENTAL

Starting materials for the preparation of EuZnIn, EuPdIn, EuPtIn, and EuAuIn were ingots of europium (Johnson, Matthey), zinc granules (Merck), palladium powder (200 mesh, Degussa), platinum powder (200 mesh, Degussa), gold wire ($\varnothing$ 2 mm, Degussa), and indium tear drops (Johnson Matthey), all with purities better than 99.9%. Pure samples of the four compounds were synthesized in sealed tantalum tubes under inert conditions as described earlier (2, 7).

The purity of the samples was checked by Guinier powder patterns using Cu$K\alpha_1$ radiation and α-quartz ($a$ = 491.30 pm, $c$ = 540.46 pm) as an internal standard. A comparison of the experimentally obtained powder diagrams with the calculated ones (8) assuming the lattice constants and atomic parameters of the previous crystallographic investigations (2, 7) showed only the Bragg reflections of the Eu*T*In compounds; no impurity lines were observed.

The 21.53 keV transition of $^{151}$Eu with an activity of 130 MBq (2% of the total activity of a $^{151}$Sm : $EuF_3$ source) was used for the Mössbauer spectroscopic experiments. The measurements were performed with a commercial helium bath cryostat. The temperature of the absorber could be varied from 4.2 to 300 K and was measured with a metallic resistance thermometer with an accuracy better than ± 0.5 K. The source was kept at room temperature. For all

[1] To whom correspondence should be addressed.



0022-4596/98 $25.00

four compounds the material for the Mössbauer spectroscopic measurements was the same as for the susceptibility and resistivity measurements. The samples were placed in thin-walled PVC containers at a thickness corresponding to about 10 mg Eu/cm$^2$.

Magnetic susceptibility measurements were performed on polycrystalline samples by use of a SQUID magnetometer (Quantum Design, Inc.) at temperatures between 4.2 and 300 K with magnetic flux densities up to 5.5 T.

Electrical resistivities were measured with a conventional four-point setup according to the van der Pauw technique (9) between 4.2 and 300 K. For EuPtIn, a small block ($0.8 \times 1.2 \times 1.8$ mm$^3$) was cut from a larger polycrystalline piece. Since the EuZnIn sample was extremely brittle, these resistivity data were measured on an irregular piece of about $1 \times 1 \times 1$ mm$^3$. Cooling and heating curves were identical within error limits for both compounds, also for different samples.

## RESULTS AND DISCUSSION

### *Crystal Chemistry*

The crystal structures of the Eu$T$In compounds are all derived from the $KHg_2$ type (4). EuZnIn adopts the $KHg_2$ type with a statistical distribution of the zinc and indium atoms on the mercury position. EuPdIn, EuPtIn, and EuAuIn crystallize with the TiNiSi structure (5), a ternary ordered version of the $KHg_2$ type. The structures of EuZnIn (7) and EuPtIn (7) are presented as examples in Fig. 1.

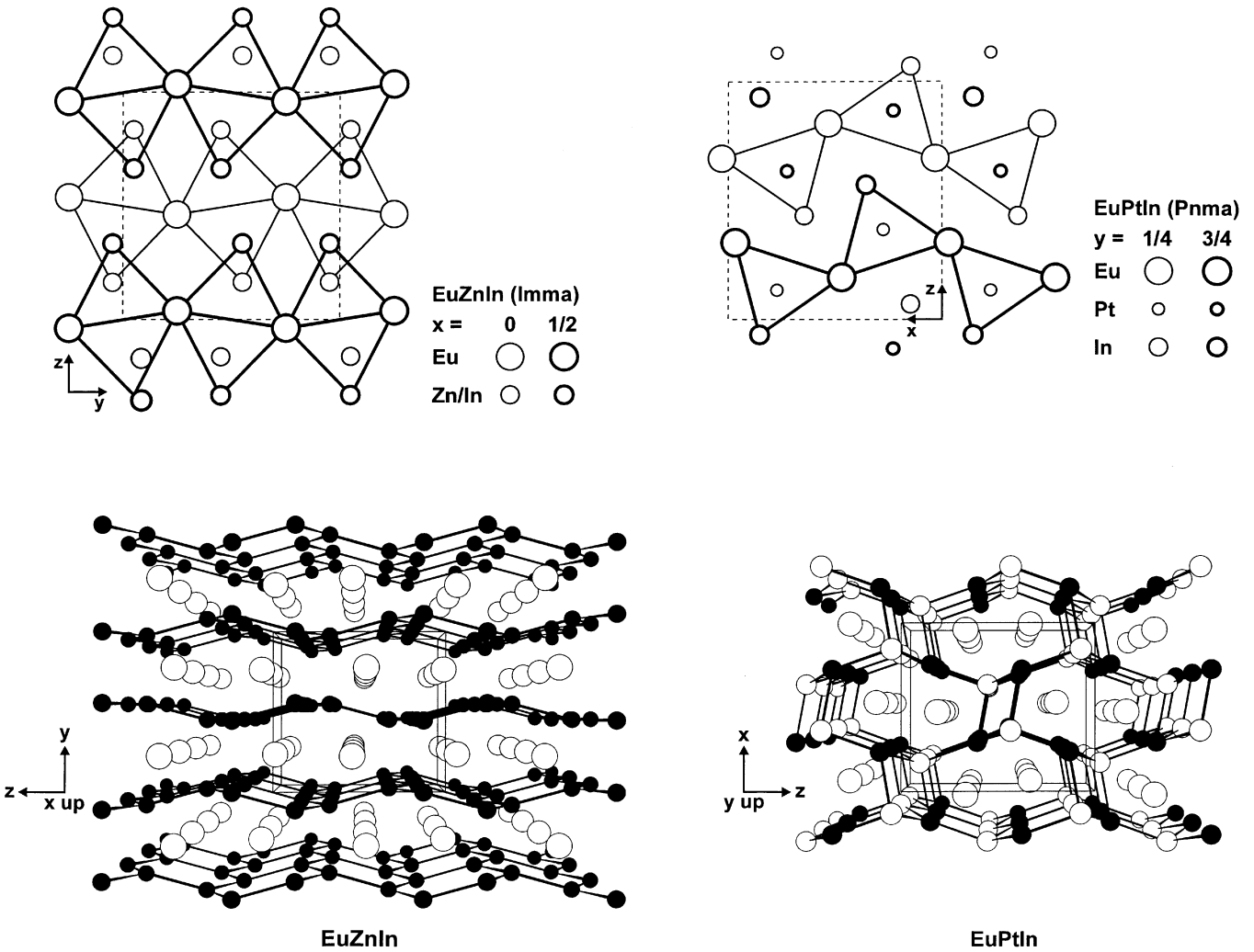


**FIG. 1.** Crystal structures of EuZnIn and EuPtIn. In the upper part of the drawing we present projections of both structures along the short axis. All atoms lie on mirror planes perpendicular to the projection direction. The trigonal double prisms in EuZnIn and the platinum-centered [$Eu_4In_2$] prisms in EuPtIn are outlined. In the lower part the two-dimensionally infinite [ZnIn] and three-dimensionally infinite [PtIn] polyanions are emphasized in perspective drawings along the same direction.

**TABLE 1**
**Crystallographic and Magnetic Data of Eu*T*In (*T* = Zn, Pd, Pt, Au)**

| Compound (Str. type) | Eu–Eu (pm) | Eu–T (pm) | Eu–In (pm) | $\mu_{exp}(\mu_B)$ | $\Theta_P$ (K) | $T_N$ (K) (Magn.) | $T_0$ (K) ($^{151}$Eu MB) | $B_{hf}$ (T) ($^{151}$Eu MB) | $B_C$ (T) at 5 K | $\mu_{sm(exp)}(\mu_B)$ (at 5.5 T) |
|---|---|---|---|---|---|---|---|---|---|---|
| EuZnIn ($KHg_2$) | $2\times395.3$<br>$2\times426.3$ | 333.0–351.7 | 333.0–351.7 | 7.80(5) | 6(2) | 8.0(5) | 9.5(5) | 20.1 | — | 4.8(1) |
| EuPdIn (TiNiSi) | $2\times379.4$<br>$2\times394.4$ | 313.7–323.2 | 338.6–358.2 | 7.6(1) | 13(1) | 13.0(5) | 15.5(5) | 22.2 | 3.1(1) | 5.9(1) |
| EuPtIn (TiNiSi) | $2\times376.1$<br>$2\times393.2$ | 311.2–322.3 | 337.8–353.1 | 8.0(1) | 20(2) | 16.0(5) | 20.0(5) | 23.1 | 1.1(1) and 2.6(2) | 7.0(1) |
| EuAuIn (TiNiSi) | $2\times390.2$<br>$2\times394.1$ | 317.1–334.1 | 336.5–351.6 | 7.5(1) | 22(1) | 21.0(5) | 20.0(5) | 21.5 | 0.25(2) | 5.9(1) |

*Note*: The magnetic data of EuPdIn and EuAuIn were taken from Ref. (7) for comparison. The shortest Eu–Eu and the varying Eu–T and Eu–In distances in the four structures are listed.

$\mu_{exp}$: experimental magnetic moment in the Curie-Weiss region; $\Theta_P$: paramagnetic Curie temperature; $T_N$: Néel temperature; $T_0$: onset of the ordering temperature determined by $^{151}$Eu Mössbauer spectroscopy; $B_{hf}$: magnetic hyperfine field determined by $^{151}$Eu Mössbauer spectroscopy; $B_C$: critical magnetic field; $\mu_{sm(exp)}$: experimental saturation magnetic moment at 5.5 T.

The europium atoms form zigzag chains running along the *y* axis (EuZnIn) and the *x* axis (EuPtIn). The intrachain Eu–Eu distances are always slightly smaller than the interchain Eu–Eu distances (see Table 1). From a geometrical point of view the europium zigzag chains form transition metal centered trigonal prisms with the indium atoms, as outlined in the upper part of Fig. 1. The trigonal prisms $[PtEu_4In_2]$ in EuPtIn point alternatingly to the $+z$ and $-z$ direction, while there is a statistical arrangement in EuZnIn with $KHg_2$ type structure. We have therefore outlined the double prisms in Fig. 1.

The strongest bonding interactions in the four compounds certainly occur between the transition metal and indium atoms, which are arranged in the form of strongly puckered $[T_3In_3]$ hexagons (lower part of Fig. 1). In the case of the EuZnIn structure, these hexagons are statistically occupied by zinc and indium atoms. The [ZnIn] polyanion in EuZnIn is essentially two-dimensional, while a three-dimensional network of corner-sharing $PtIn_4$ tetrahedra is present in EuPtIn. A more detailed description of the crystal chemistry of these compounds is given in Ref. (2).

### *Magnetic and Electrical Properties*

Susceptibility, magnetization, and electrical resistivity data for EuPdIn and EuAuIn have already been reported in Ref. (7). Both compounds are metamagnets. The relevant magnetic data for EuPdIn and EuAuIn are listed in Table 1 for comparison.

Plots of the inverse magnetic susceptibility of EuZnIn and EuPtIn are shown in Fig. 2. EuPtIn shows Curie-Weiss behavior above 60 K. The experimental magnetic moment of $\mu_{exp} = 8.0(1)\,\mu_B$/Eu was obtained from a fit of the $1/\chi$ vs T plot (data above 60 K) according to the modified Curie-Weiss law $\chi = \chi_0 + C/(T - \Theta)$. This magnetic moment is close to the free ion value of $\mu_{eff} = 7.94\,\mu_B$ for $Eu^{2+}$. The paramagnetic Curie temperature (Weiss constant) amounts to $\Theta = 20(2)$ K and the temperature independent contribution was $\chi_0 = 11(1)\times10^{-9}$ m$^3$/mol. EuPtIn orders antiferromagnetically at 16.0(5) K when measured with an external magnetic flux density of 0.5 T (inset of Fig. 2). A second, small anomaly is observed at 10.0(5) K. The magnetization vs external magnetic field behavior of EuPtIn is presented in Fig. 3. At 50 K the magnetization curve is almost linear as is usual for a paramagnetic compound. At 5 K and low flux densities the magnetization increases monotonically as expected for an antiferromagnet. A first metamagnetic transition (antiferromagnetic-to-ferromagnetic spin alignment) is observed at a critical field strength of 1.1(1) T, followed by a second transition at 2.6(2) T. EuPtIn may therefore be characterized as a two-step metamagnet. At the highest obtainable field strength of 5.5 T the saturation magnetic moment amounts to $\mu_{sm(exp)} = 7.0(1)\,\mu_B$/Eu, in agreement with the calculated value of $\mu_{sm(calc)} = 7.0\,\mu_B$/Eu according to $\mu_{sm(calc)} = g\times J\,\mu_B$ (10). Thus all magnetic moments are ordered parallel at 5 K and 5.5 T. The data at 14 K show only one transition at about 1.0(1) T and a saturation magnetic moment of $\mu_{sm(exp)} = 5.9(1)\,\mu_B$/Eu at 5.5 T. The second step observed in the 5 K data most likely arises from the 10 K anomaly. All other Eu*TX* (*T* = Cu, Zn, Pd, Ag, Pt, Au; *X* = Ge, In, Sn) compounds show only single-step magnetization behavior (7, 11, 12).

The $1/\chi$ vs T plot for EuZnIn (Fig. 2) shows a slight curvature. A fit of the data above 60 K according to $\chi = \chi_0 + C/(T - \Theta)$ resulted in a temperature independent contribution $\chi_0 = 24(1)\times10^{-9}$ m$^3$/mol, a paramagnetic Curie temperature of $\Theta = 6(2)$ K, and a magnetic moment

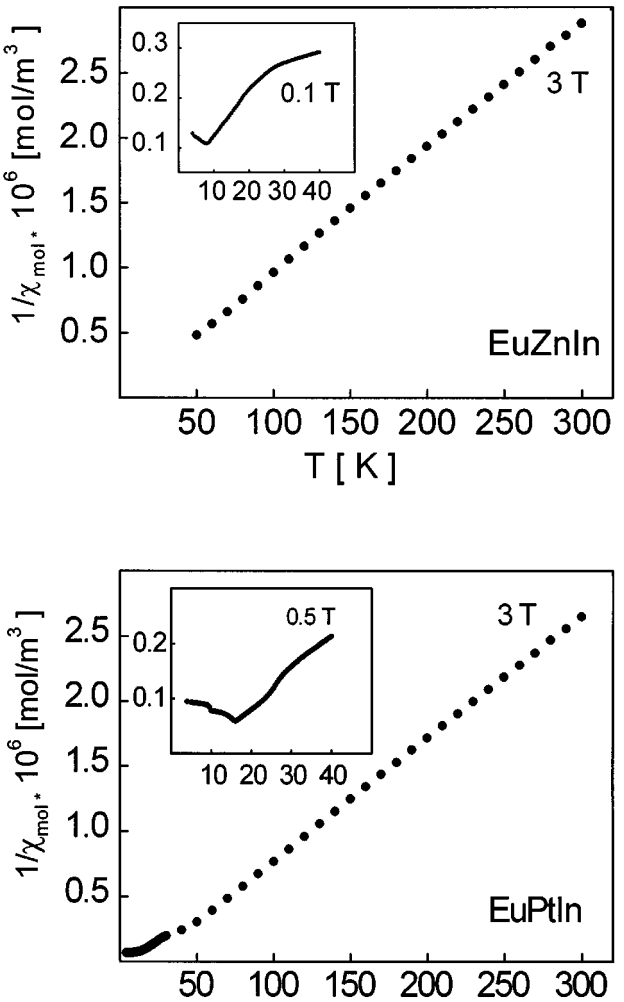


FIG. 2. Temperature dependence of the inverse magnetic susceptibility of EuZnIn and EuPtIn measured at varying flux densities.

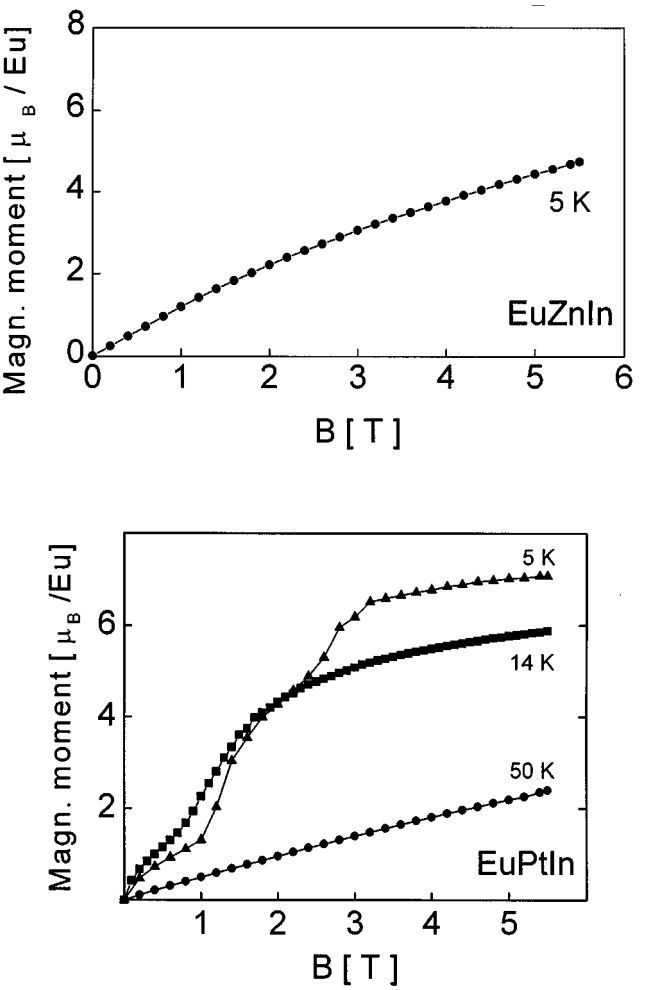


FIG. 3. Magnetization vs external magnetic flux density for EuZnIn and EuPtIn at various temperatures.

of $\mu_{exp} = 7.80(5)\,\mu_B$/Eu, indicating divalent europium. The temperature independent term $\chi_0$ includes, among other things, the Pauli contribution of the conduction electrons. EuZnIn orders antiferromagnetically at 8.0(5) K (inset of Fig. 2). No field induced transition is evident from the magnetization vs external field plot (Fig. 3). The magnetization increases monotonically with increasing magnetic field. At 5.5 T the magnetic moment amounts to $\mu_{sm(exp)} = 4.8(1)\,\mu_B$/Eu.

The temperature dependence of the electrical resistivity of EuZnIn and EuPtIn is shown in Fig. 4. Absolute values for plotted for EuPtIn, while only the resistance ratio R/R(300 K) is plotted for EuZnIn. The polycrystalline broken pieces of the EuZnIn sample were too brittle to be cut into regular shaped blocks of defined dimensions. The resistance of both compounds decreases more or less monotonically from 300 to 40 K as is typical for metallic conductors. The specific resistivity of EuPtIn at room temperature amounts to 490 μΩcm. In both plots anomalies are observed at low temperatures. Below about 9 K (EuZnIn) and 23 K (EuPtIn), the resistivity plots show a slightly different slope, most likely due to freezing of spin-disorder scattering in the magnetically ordered state. These transition temperatures are in good agreement with the magnetic data discussed above.

### $^{151}$*Eu Mössbauer Spectroscopy*

In Figs. 5–8 the Mössbauer spectra are shown at 78 K, at a temperature just below $T_N$, and at 4.2 K, together with transmission integral fits. The fitting parameters and the results at some additional temperatures are listed in Table 2. In all spectra an impurity of Eu(III), which is included in the fits by a simple Lorentzian component but not reported in the tables, can be located near $\delta \approx 1$ mm s$^{-1}$. The fractional area of this component

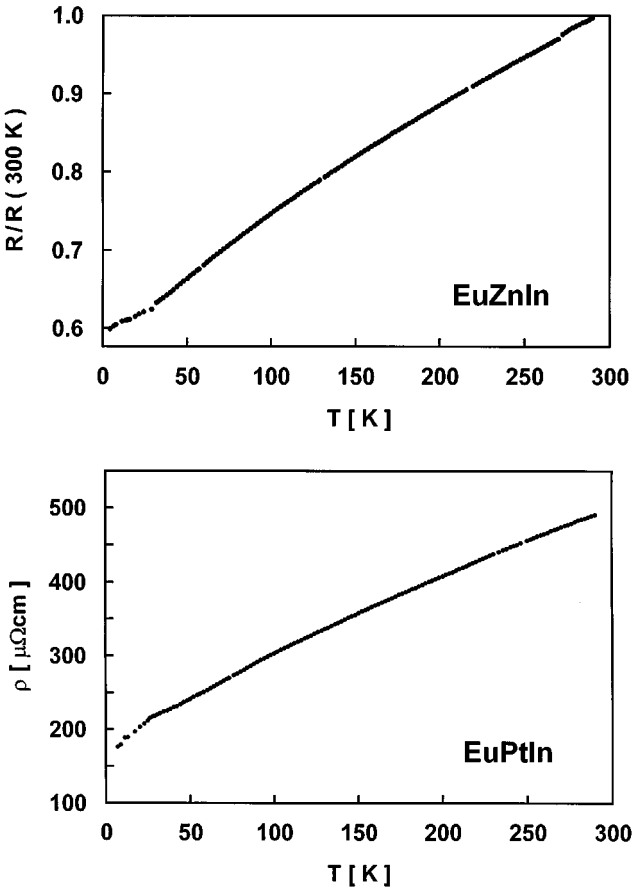


**FIG. 4.** Temperature dependence of the electrical resistivities of EuZnIn and EuPtIn.

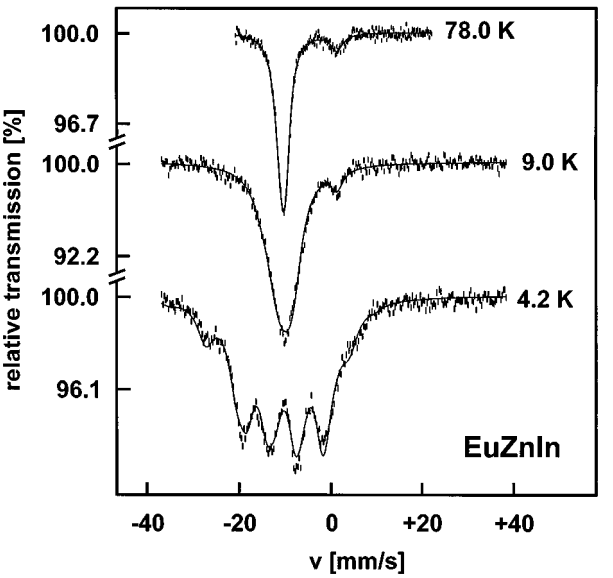


**FIG. 5.** Experimental and simulated $^{151}$Eu Mössbauer spectra of EuZnIn.

just above $T_N$ is 7% for EuZnIn and 5% for the other compounds.

Above $T_N$ the main spectral components of all compounds are well reproduced by a single Eu(II) site subjected to an axially symmetric electrical field gradient ($\eta = 0$). However, the isomer shifts reveal large differences over a range of 1.5 mm s$^{-1}$. Figure 9 shows that the isomer shift for the three isostructural compounds EuPdIn, EuPtIn, and EuAuIn can be linearly correlated with the shortest Eu–Eu distance in the structure. The correlation even includes the compound EuZnIn despite the Zn/In disorder in the latter.

For all compounds the onset of antiferromagnetic ordering is reflected in the appearance of magnetic hyperfine splitting. The Néel temperatures observed in the Mössbauer spectra are close to those extracted from the magnetic susceptibility measurements. Like the isomer shift, the saturation value of the magnetic flux density represented by its value at 4.2 K can also be almost linearly correlated with the shortest Eu–Eu distance (see Fig. 9).

Asymmetry in the observed magnetically split spectra reveals the necessity to include the nuclear electrical quadrupole interaction in the Hamiltonians. In EuPdIn, $\Delta E_Q$ changes from 10 to $-2$ mm s$^{-1}$ when magnetic order is established. This can be attributed to an angle of about 60° between the axis of the principal component $V_{zz}$ of the electric field gradient and the magnetic flux density. In the other compounds the principal axis of the EFG is parallel to the magnetic flux density.

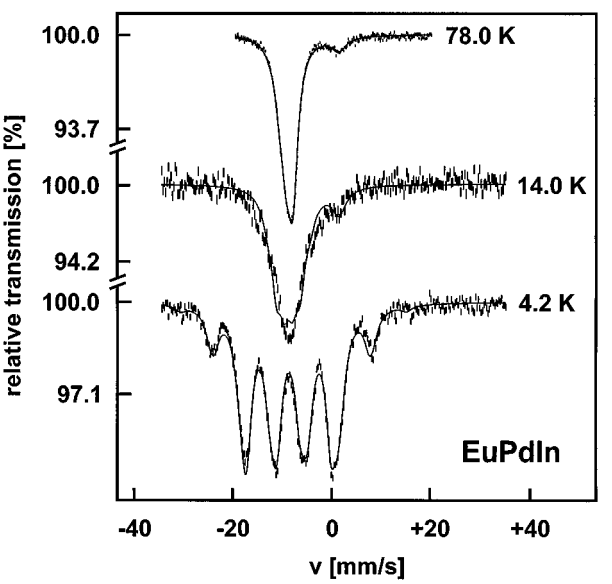


**FIG. 6.** Experimental and simulated $^{151}$Eu Mössbauer spectra of EuPdIn.

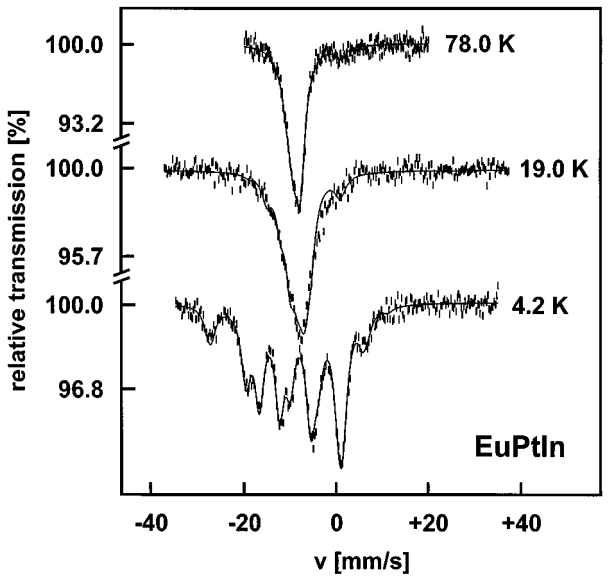


**FIG. 7.** Experimental and simulated $^{151}$Eu Mössbauer spectra of EuPtIn.

The hyperfine split spectra could be fitted to individual Lorentzian components of 2.3 mm s$^{-1}$ width. This width is close to the natural linewidth of $^{151}$Eu, indicating the presence of single Mössbauer sites. The only exception of EuZnIn, in which below $T_N$ an increased Lorentzian linewidth of 3.8 mm s$^{-1}$ had to be used to obtain satisfactory fits. This effect is also apparent from visual inspection of Fig. 5. The excess linewidth can be attributed to a distribution of the magnetic field orientation and/or magnitude. Site distribution effects are indeed expected to be present in EuZnIn from its crystal structure, where Zn and In atoms are distributed statistically around the Eu positions. Evidently, the isomer shift and the nuclear electric quadrupolar interaction are too similar to resolve the different sites by $^{151}$Eu-Mössbauer spectroscopy in the spectra above $T_N$. Thus it appears that in these compounds the magnetically hyperfine splitting patterns are the most sensitive indicators of site inequivalence.

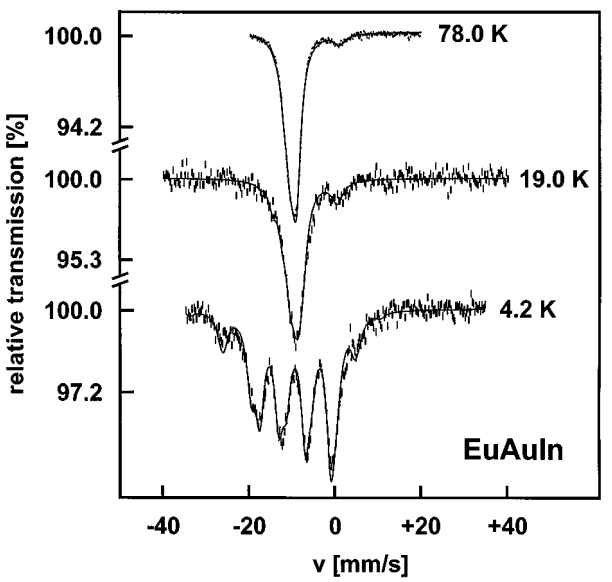


**FIG. 8.** Experimental and simulated $^{151}$Eu Mössbauer spectra of EuAuIn.

**TABLE 2**
**$^{151}$Eu Mössbauer Fitting Parameters for Eu$T$In ($T$ = Zn, Pd, Pt, Au) as a Function of Temperature**

| $T$ ($K$) | $\delta$ (mm/s) | $W$ (mm/s) | $\Delta E_Q$ (mm/s) | $\lvert B\rvert$ (T) |
|---|---|---|---|---|
| | | EuZnIn | | |
| 300 | − 10.4(1) | 2.0(4) | 6(2) | — |
| 78.0 | − 10.25(4) | 2.2(2) | 6(1) | — |
| 11.0 | − 10.26(7) | 2.3(3) | 5(2) | — |
| 10.0 | − 10.25(4) | 2.3(1) | 5 | — |
| 9.0 | − 10.2(1) | 3.8 | 5 | 4.4(4) |
| 4.2 | − 10.27(9) | 3.8(3) | 5 | 20.1(3) |
| | | EuPdIn | | |
| 300 | − 9.4(1) | 2.3(2) | 10(1) | — |
| 78.0 | − 9.0(1) | 2.3(1) | 10(1) | — |
| 16.0 | − 9.0(1) | 2.3 | 10 | — |
| 15.0 | − 9.0(1) | 4.1(3) | − 2 | 1.8(6) |
| 14.0 | − 9.0(2) | 4.7(9) | − 2 | 4.5(9) |
| 10.0 | − 8.8(2) | 2.9(2) | − 2 | 18.2(2) |
| 4.2 | − 8.8(1) | 2.4(1) | − 2(1) | 22.2(1) |
| | | EuAuIn | | |
| 300 | − 10.2(1) | 2.3(3) | 10(1) | — |
| 78.0 | − 9.9(1) | 2.2(7) | 10(1) | — |
| 35.0 | − 9.7(1) | 2.3(4) | 9(2) | — |
| 30.0 | − 9.7(1) | 2.3(4) | 9(2) | — |
| 20.0 | − 9.8(1) | 2.3 | 9 | 2.5(7) |
| 19.0 | − 9.8(1) | 2.3 | 9 | 4.2(4) |
| 15.0 | − 9.7(1) | 2.3 | 9 | 19.7(4) |
| 10.0 | − 9.8(1) | 2.3 | 9(1) | 20.1(2) |
| 4.2 | − 9.7(4) | 2.3 | 8(1) | 21.5(2) |
| | | EuPtIn | | |
| 300 | − 8.86(8) | 2.3(3) | 10(1) | — |
| 78.0 | − 8.75(8) | 2.3 | 10(1) | — |
| 21.0 | − 8.64(8) | 2.3(2) | 10 | — |
| 20.0 | − 8.6(1) | 2.3 | 10 | 2.2(7) |
| 19.0 | − 8.6(1) | 2.3 | 10 | 5.9(3) |
| 15.0 | − 8.63(7) | 2.3 | 10 | 19.2(2) |
| 10.0 | − 8.62(7) | 2.3 | 9(1) | 21.8(2) |
| 4.2 | − 8.66(7) | 2.3 | 10(1) | 23.1(2) |

*Note*: The numbers in parentheses give the statistical errors in the last digit. Values without parentheses were kept fixed by the fitting program.
$\delta$, isomer shift with respect to $EuF_3$; $W$, experimental linewidth; $\Delta E_Q$, electric quadrupole interaction; $B$, static magnetic flux density.

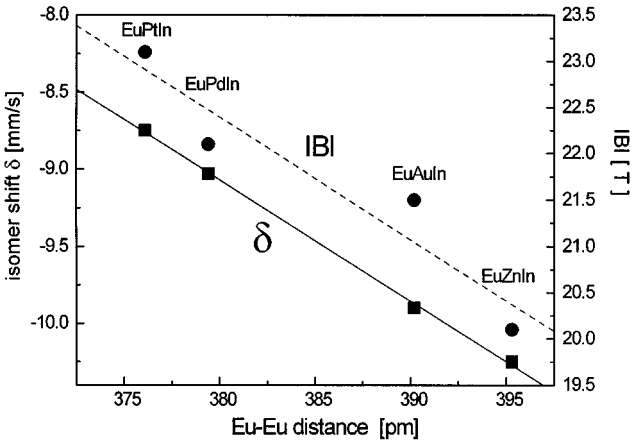


**FIG. 9.** Correlation between the shortest Eu–Eu distance and the isomer shift $\delta$ at 78 K (■) and the magnetic flux density $|B|$ at 4.2 K (●) for EuZnIn, EuPdIn, EuPtIn, and EuAuIn, respectively.

## ACKNOWLEDGMENTS

G.K. thanks Prof. Wolfgang Jeitschko for helpful discussions. We are also indebted to Nicola Rollbühler and Dr. Reinhard K. Kremer for the resistivity measurements and to Dr. Wolfgang Gerhartz (Degussa AG) for a generous gift of palladium powder, platinum powder, and gold wire. This work was financially supported by the Deutsche Forschungsgemeinschaft (Po 573/1-1) and the Fonds der Chemischen Industrie.

## REFERENCES

1. R. Müllmann, B. D. Mosel, H. Eckert, R. Pöttgen, and R. K. Kremer, *Hyperfine. Interact.* **108,** 389 (1997).
2. R. Pöttgen, *Z. Kristallogr.* **211,** 884 (1996).
3. R. Pöttgen, R.-D. Hoffmann, R. Müllmann, B. D. Mosel, and G. Kotzyba, *Chem. Eur. J.* **3,** 1852 (1997).
4. E. J. Duwell and N. C. Baenziger, *Acta Crystallogr.* **8,** 705 (1955).
5. C. B. Shoemaker and D. P. Shoemaker, *Acta Crystallogr.* **18,** 900 (1965).
6. R. Pöttgen, *J. Mater. Chem.* **5,** 505 (1995).
7. R. Pöttgen, *J. Mater. Chem.* **6,** 63 (1996).
8. K. Yvon, W. Jeitschko, and E. Parthé, *J. Appl. Crystallogr.* **10,** 73 (1977).
9. L. J. van der Pauw, *Philips Res. Rep.* **13,** 1 (1958).
10. A. Szytuła and J. Leciejewicz, "Handbook of Crystal Structures and Magnetic Properties of Rare Earth Intermetallics." CRC Press, Boca Raton, Florida, 1994.
11. C. Tomuschat and H.-U. Schuster, *Z. Anorg. Allg. Chem.* **518,** 161 (1984).
12. R. Pöttgen, *Z. Kristallogr.* **210,** 924 (1996).